THE RICE UNIVERSITY CCD IMAGER FOR GAMMA-RAY BURST STUDIES[1]

Ian A. Smith, Reginald J. Dufour, Edison P. Liang
Rice University, Department of Physics and Astronomy
6100 South Main, MS 108, Houston, TX, 77251–1892
Email: iansmith@rice.edu

Jeffrey M. Silverman
Astronomy Department, University of California at Berkeley
Berkeley, CA 94720–3411

Larry C. Hardin, Robert D. Forgey
Hardin Optical Company, P.O. Box 219, Bandon, OR 97411
http://www.hardin-optical.com/

Mark A. Skinner, Andrew Alday
Boeing LTS, Inc., 535 Lipoa Parkway, Ste. 200, Kihei, Maui, HI 96753

Carl Akerlof, Heather Swan, Tim McKay, Eli Rykoff, Sarah Yost
University of Michigan, 2477 Randall Laboratory
450 Church Street, Ann Arbor, MI 48109

Gamma-Ray Bursts (GRBs) are the largest explosions in the Universe since the Big Bang. The ability to study GRBs has significantly improved thanks to the rapid localization of bursts by the *Swift* satellite. The AEOS 3.63-m telescope is filling important gaps in the capabilities of the world-wide network of ground-based observatories doing GRB follow-up observations. Here we summarize the status of the field and some of the results obtained by the Rice University CCD imager (RUCCD), one of the instruments used by the MARGE collaboration to study burst afterglows. The RUCCD currently operates in Coudé room 6 of the AEOS telescope. It has eight filter wheel slots, and can perform imaging photometry, spectroscopy, and polarimetry, using exposure times as short as 20 milliseconds. The CCD has a high quality and uniformity, and the focus is good across the whole field of view. Spectroscopy is performed using an imaging-grism and/or imaging-grating system rather than a slit spectrometer. This disperses the spectra of all the sources in the field of view. During the times it is installed in the Coudé room, the RUCCD is thermoelectrically cooled, and is in a permanent state of readiness for making observations.

1. INTRODUCTION

A gamma-ray burst (GRB) is a short, bright, unpredictable flash of gamma-rays. For historical reviews see [1, 2, 3].

Since their discovery in 1967 by the Vela satellites [4], GRBs have remained one of the greatest modern astrophysical mysteries. Historically, they have been hard to study because of their short duration, their unpredictably random appearance in space and time, their lack of burst repetition, and the problems with obtaining accurate locations using gamma-ray imaging.

1.1 The *Swift* Satellite

The study of GRBs has improved significantly thanks to the *Swift* satellite [5]. *Swift* is a NASA MIDEX mission dedicated to studying GRBs. It was successfully launched on November 20, 2004, and became fully operational in 2005. The on-board gamma-ray Burst Alert (BAT), X-Ray (XRT), and UV-Optical (UVOT) Telescopes are all performing well.

When the BAT detects a GRB, its gamma-ray imaging capability allows it to determine the burst location to within a few arcminutes. The satellite then slews rapidly so that the XRT and UVOT can study the region to look for a new transient source. If an X-ray counterpart is present, coordinates with an accuracy

[1]Based on observations made at the Maui Space Surveillance System operated by Detachment 15 of the US Air Force Research Laboratory's Directed Energy Directorate.

of $< 10''$ are determined ~ 100 seconds after the burst. If an optical counterpart is present, coordinates with an accuracy of $\sim 0.3''$ are determined ~ 4 minutes after the burst. The results found by the three instruments are rapidly broadcasted to other researchers via the GRB Coordinates Network (GCN) [6]. This allows ground-based optical and radio telescopes to join the search for and study of the multiwavelength emission.

Swift is currently locating an average of ~ 2 bursts per week. These come at truly random intervals. For example, from 2005 June 7 to 2005 July 12, BAT saw only 1 burst. But in the next 5 days it saw 7!

For the first time, *Swift* has been able to accurately localize a few short bursts – that emit gamma-rays for less than ~ 1 second – as well as the better studied long bursts that can last up to several minutes [7]. One of the surprising results from *Swift* is that these two classes of bursts may have different progenitors.

1.2 Counterparts

During the burst, it is believed that most of the electromagnetic energy is released in gamma-rays. However, the study of GRBs has improved dramatically since 1997 through the study of their multiwavelength counterparts.

Fading X-ray counterparts have been found for almost all the bursts that have had rapid X-ray observations. The rapid slewing capabilities of *Swift* has allowed it to study for the first time the X-ray emission all the way from the tail end of the burst emission. One of the surprises found by *Swift* is the significant variability of the early X-ray emission in many bursts [8]. Bright X-ray flares have been seen after some GRBs, including a giant flare a few minutes after GRB 050502B that was comparable in total energy to the burst itself. These X-ray flares suggest that the central engines of some bursts may have longer periods of activity than was previously inferred from the gamma-ray emission alone.

Searches for optical counterparts are made by comparing new images taken at different times and by comparing with pre-existing catalogs and archival plates. Starting with GRB 970228 [9], optical transients have been found to many but not all of the bursts with fading X-ray counterparts.

1.3 Redshifts and Energetics

By studying the emission and absorption lines in the afterglow and/or host galaxy spectra, the redshifts (or their lower limits) have been determined for many of the bursts. A wide range of redshifts have been found, as high as $z = 6.295$ for GRB 050904 [10].

The fact that most of the bursts are at large cosmological distances implies they are the most powerful explosions known in the Universe. If radiated isotropically, the non-thermal gamma-ray emission during the burst would be over 10^{53} ergs in some cases. This is already significantly more energy than is released in regular supernova explosions. The extreme energetics are reduced somewhat due to the expected beaming in the burst [11]. However, this implies that there must be many more bursts occurring throughout the Universe that we miss because we are not in the line-of-sight of the beam.

1.4 Models for Long-Duration Bursts

Observations of new bursts are continuing to produce surprises, and there is much left to learn. However, the current evidence indicates that at least some of the long-duration GRBs are due to the explosive collapse of massive stars.

Figure 1 illustrates the qualitative "fireball" model for GRBs. During and after the burst, the observed multiwavelength emission comes from several distinct components. The explosion produces shocks that energize particles whose radiation gives the "prompt" bright burst emission. A reverse shock can give an optical and/or radio "flash." The later "afterglow" emission comes from an expanding fireball as it sweeps up the surrounding medium. At later times, signatures may appear that are characteristic of supernovae or hypernovae. Hypernovae have broad spectral features suggesting large ejecta velocities and large explosion energies. For example, the supernova SN 2003dh associated with GRB 030329 strongly resembled the Type 1c hypernovae SN 1997ef and SN 1998bw [13, 14]. Finally, a "quiescent" constant emission comes from any underlying host galaxy after the afterglow has faded away, days or weeks after the burst.

Since GRBs can be seen to very large distances, and since massive stars have short lifetimes, GRBs could provide an important way to study star formation and death throughout the Universe, and thus processes such as the creation of heavy elements and cosmic ray acceleration.

1.5 Models for Short-Duration Bursts

While some of the short-duration GRBs may also be the result of the explosive collapse of massive stars, the

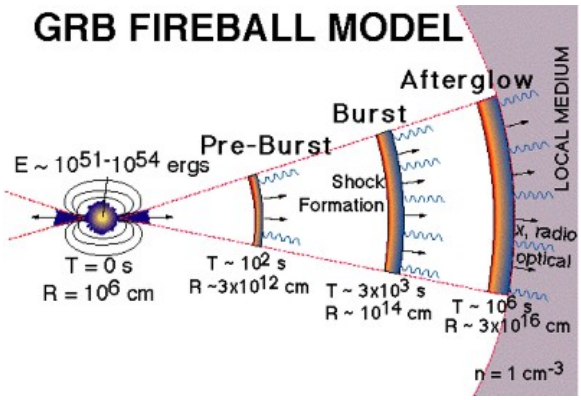

Figure 1: The qualitative fireball model for GRBs. Figure courtesy of the *Swift* web page [12].

lack of detection of supernova or hypernova signatures in some nearby short bursts indicates that these may have different progenitors.

One possibility is that they may be due to the merger of two neutron stars in an inspiralling binary system. These systems are old and will normally be located in low density environments. They are therefore expected to produce a bright prompt emission, but little afterglow [15].

Another possibility is that they may be due to giant flares from magnetars. These highly magnetized neutron stars produce occasional bursts that are extremely bright. For example, one of the first bursts seen by *Swift* was a giant flare on 27 December 2004 emitted by the magnetar SGR 1806–20 [16]. However, this may only be able to account for a relatively small fraction of the short bursts [17].

2. OUTSTANDING QUESTIONS

Despite the recent progress, many fundamental questions remain about GRBs. The following outlines some of the outstanding issues. These can be addressed by continued observations of new GRBs.

- What is the physics behind the short-duration bursts?
- Why is the afterglow decay complex in some bursts, such as in GRB 030329? For this burst, a bright new $R \sim 12$ optical source was found an hour after the burst whose optical decay contained several breaks and bumps; see Figure 2. It is of interest to similarly study the afterglow evolution in the earliest stages of the fireball.
- What is the high time resolution evolution of the optical emission for those bursts with bright prompt optical emission such as GRB 990123 [19], GRB 041219a [20], and GRB 050904 [21]? How does the optical evolution correlate with the gamma-ray spectrum, as illustrated in Figure 3?
- What is the polarization of the early emission and how does it evolve with time? It is plausible that the prompt and/or afterglow emission could be highly polarized, either due to large-scale persistent magnetic fields, or because of the asymmetry in the way that the beamed fireball is viewed from off-axis. A very large polarization ($\sim 80\%$) claimed for the prompt gamma-ray emission in GRB 021206 [23] has been disputed [24]. Optical observations of the afterglows of a few GRBs starting hours to days after the burst have measured polarizations that can be variable and that are $\lesssim 3\%$, for example [25, 26, 27, 28]. It is of particular interest to perform optical polarimetry as soon as possible after the burst to study its very early evolution.
- How does the spectral shape evolve in the early afterglow? The afterglow spectrum can contain several breaks due to various physical processes, and the wavelengths of these spectral breaks evolve with time.
- Some of the long bursts have very soft prompt emission, and these have been called X-Ray Flashes (XRFs; [29]). These may be the same phenomenon as regular GRBs, except that we are viewing them from an angle that is off the axis of the beam of the energetic particles produced in the explosion [30].

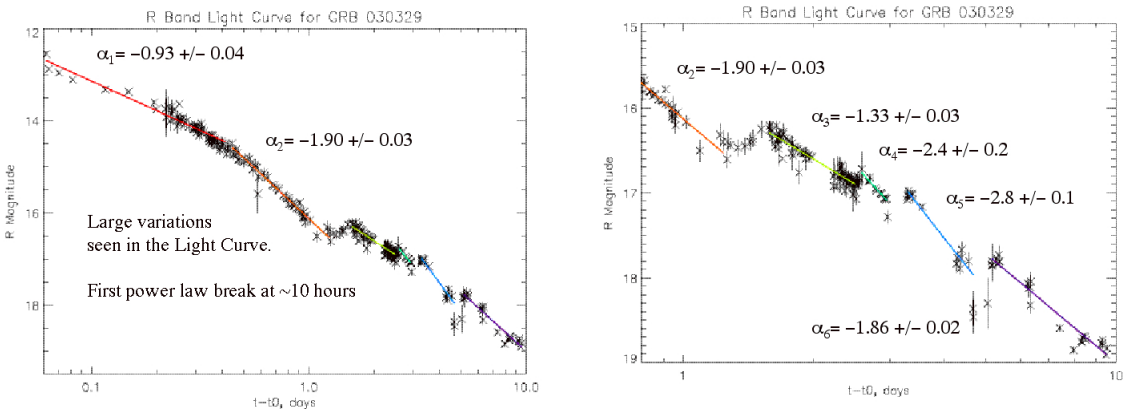

Figure 2: The R-band light curve for the decay of the optical afterglow to GRB 030329 in the days following the burst. The light curve is remarkably complex. Figure courtesy of the HETE web page [18].

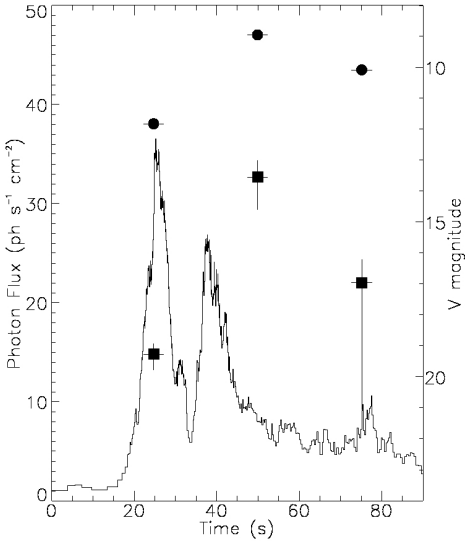

Figure 3: The light curves for GRB 990123. The histogram shows the gamma-ray light curve integrated over a broad energy band. The circles show the optical observations; these do not appear to correlate with the gamma-ray flux. The squares show extrapolations to the V-band for the gamma-ray spectra at the times of the optical observations; these do appear to correlate with the measured optical fluxes [22].

3. THE RICE UNIVERSITY CCD IMAGER (RUCCD)

Despite the excellent capabilities *Swift*, the onboard UVOT has some important limitations. It has a relatively small aperture, has no polarimetric capabilities, and for every burst it must complete its primary list of pre-planned observations and distribute finding charts to ground-based observers before it can do any flexible observations. Therefore, the *Swift* mission can be ideally complemented by observations using a rapidly-slewing large-aperture telescope with adaptable instrumentation. Such observations can be performed by the AEOS 3.63-m telescope (Haleakala, Maui, HI).

The AEOS telescope slews very rapidly: 17.6 deg/sec in azimuth and 4.75 deg/sec in elevation [31]. Thus a target can be reliably acquired in just a few seconds after the decision to repoint has been made, i.e. within a minute or so of the GRB detection by the satellite. Given the brevity of the burst, the rapid and reliable target acquisition makes AEOS uniquely qualified to study the early GRB emissions with a large-aperture telescope.

The AEOS telescope currently has two instruments dedicated to studying GRBs. These instruments form the MARGE burst system. The AEOS Burst Camera is described by Akerlof et al. [32]. Here we describe the Rice University CCD imager (**RUCCD**).

The RUCCD is shown in Figure 4. The aim was to build a versatile instrument that can perform a wide range of observations and remain at the cutting edge, even as the field evolves. The equipment has proven

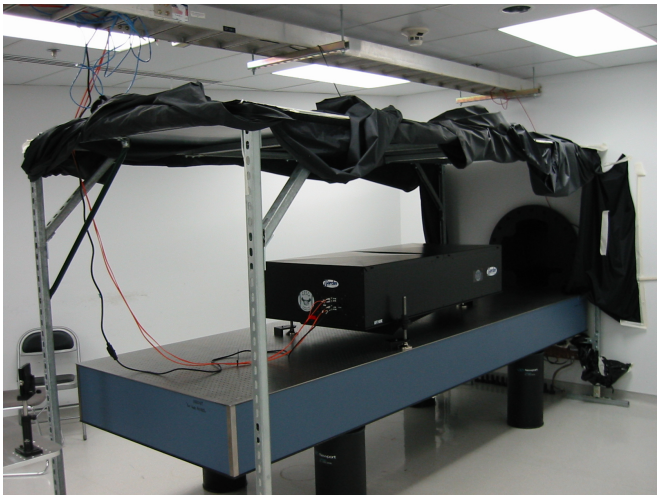

Figure 4: The RUCCD set up on the optical bench in Coudé room 6 of the AEOS telescope.

to be very robust. The only thing that has broken so far is an external hard drive.

The RUCCD was successfully installed and aligned in Coudé room 6 of the AEOS telescope for the first time on 2004 February 3–4. The smooth installation and operation of the RUCCD has been made possible through the extensive efforts and cooperation of the staff at the telescope, and we would like to thank everyone who has spent time helping us.

Since Coudé room 6 is shared with other Visiting Experiments, the RUCCD is not installed all the time. It has generally been available in blocks of a few months totalling $\sim 1/2$ of the year. Re-installation of the RUCCD is straightforward since all the opto-mechanical parts are in one enclosed assembly; see Figure 4. This makes the instrument effectively plug-and-play. The only cables connecting the box to the outside are a 110V power line and two fiber optics communication lines that are used to control the filter wheel and CCD. Since our mount model is now permanently stored in the telescope control computer, it does not require much observing time to update the model and focus settings each time the RUCCD is re-installed.

3.1 Optical Assembly (OA)

The current configuration is optimized to operate at the f/200 Coudé focus. The optical assembly (OA) was developed by Hardin Optical Company of Bandon, OR [33]. The OA contains a two-mirror off-axis focal reducing system. This configuration avoids having blind spots in the CCD field; since we may not know the accurate location of the GRB initially, having a blind spot would not be acceptable. To simplify the fabrication and costs and timeline, we have used a spherical concave mirror coupled with a beam folding flat mirror. This still gives near diffraction-limited performance over the entire field-of-view of the CCD. As we show in our sample images, the OA is working extremely well; the images are sharp and the field uniform over the entire FOV.

The entire housing is mounted on the Coudé room optical bench with adjusting screws for moving the assembly on the vertical axis. This allows fine tuning of the optical alignment. The mirrors can be translated in two axes (mirror separation distance and horizontal translation) for focusing and optical path centering. In practice, this internal focusing capability has not been needed; the focus has been easily obtained using the telescope alone.

The OA reduces the effective focal length of the f/200 AEOS telescope to 130 meters, or f/35.4, at the surface of the CCD. This gives an expected plate scale of 1.58 arcsec/mm and a field size of $45.3''$ on a side across the 28.7 mm square CCD chip. (The $64''$ across the diagonal of the chip is slightly larger than the $57''$ diameter beam size from the telescope through the Coudé port). This has been confirmed by our calibration observations. We measured the field size to be $46''$ on a side based on the angular separation of the Trapezium stars in the Orion Nebula (which is shown in Figure 5).

3.2 CCD Camera

The RUCCD detector is a front-illuminated 2048×2048 CCD with 14×14 micron pixels, model TH7899M

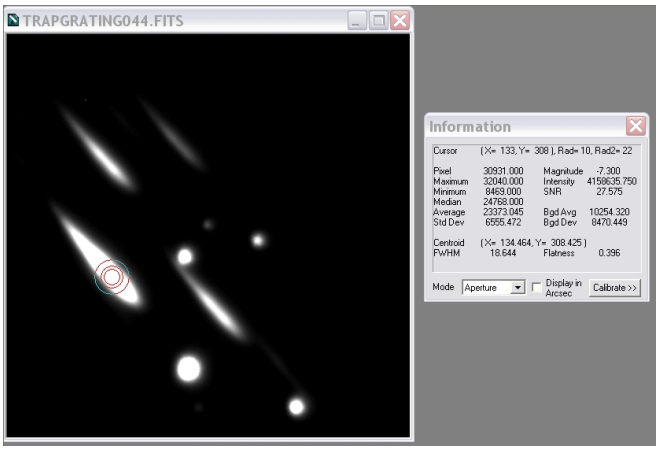

Figure 5: RUCCD grating image of the Trapezium stars in the Orion Nebula taken UT 2004-02-07:09:00:55. This is a raw image, with no data processing except for the 4×4 binning that was done in the camera. The exposure time was 0.5 seconds. The spectra of each of the stars is dispersed towards the top left corner of the image in the East–West direction; North is towards the top right corner. The Information panel is being used by the operator to check whether the spectrum is saturated. The circular cursor is moved along the spectrum. If the Maximum value exceeds 65535, the spectrum is saturated, and it needs to be redone using a shorter exposure time.

from the Atmel Corporation of San Jose, CA [34]. The peak quantum efficiency of the chip is 38% at 720 nm, and it is above 5% from $\sim$ 450 to 1020 nm. The Grade H CCD has a very high quality, with only a couple of bad pixels and a good uniformity across the whole field of view. This is very important for studying GRBs, since we may not have the opportunity to place the target on a good portion of the chip.

The CCD is housed in the Alta E10 camera system from Apogee Instruments Inc. of Auburn, CA [35]. During the times it is installed, the RUCCD is thermoelectrically cooled and is in a permanent state of readiness for making GRB observations. The camera can be cooled to 45 C below the ambient temperature, with a temperature stability of ± 0.1 C.

The shutter is a 45 mm Vincent Uniblitz precision low vibration shutter. The flexible exposure time – with exposures as short as 20 milliseconds – permits the study of both bright rapidly variable objects and faint sources using the same instrument.

The CCD is controlled through a standard 100BaseT ethernet connection. This is connected to our computer in the AEOS control room via an optical fiber.

Processing can be performed by the camera before reading out the image. Thus in addition to full-frame imaging, it is possible to do sub-frame imaging and binning up to 10×2048. This allows the option of only reading out the image in the region around the target, which increases the camera throughput speed and decreases the disk storage requirements. We normally use 10×10 binning for our point-source broad-band imaging, and 4×4 binning for our imaging spectroscopy.

3.3 Filter Wheel

The automated filter wheel for the RUCCD is Model FW-82 from DFM Engineering, Inc. of Longmont, CO [36]. It has its own onboard microprocessor and absolute encoder which is commanded via an optical fiber by our computer in the AEOS control room. The filter wheel has ports for eight 50 mm diameter round filters. The current configuration is:

- Three slots are filled by wide-band Cousins/Bessell VRI filters from Optec, Inc. of Lowell, MI [37]; we have also tried using a B filter, but found it to be less sensitive.
- Three slots are filled with Tech Spec linear glass polarizers from Edmund Scientific of Barrington, NJ [38]. These are rotated at 0, 60, and 120 degrees. Each polarizer has an IR blocking filter from Optec, Inc. to cut off the light beyond 740 nm to maximize the polarization efficiency.
- One slot is filled with a 300 g/mm plano ruled transmission grism blazed at 490 nm, number 806R from Spectra-Physics of Rochester, NY [39]. The final slot contains a 300g/mm transmission grating blazed near 500 nm. The spectral resolutions are $R \sim 10$. The strength of using the imaging-grism or imaging-grating system rather than a slit spectrometer is that it disperses the spectra of all the sources in the field of view. This is important for GRB studies, since we may not know initially which source in the field of view is the correct counterpart.

3.4 Instrument Operation and Control

Commands to the filter wheel and the CCD are integrated together via the MaxIm DL [40] software package that is running under Microsoft Windows on a PC in the AEOS control room. The familiar Windows interface makes it easy for the telescope operators to learn how to control the instrument.

The GRB and calibration observations are performed in coordination with Rice astronomers over the telephone. The operators report back what they are seeing on the screen. MaxIm DL has image analysis tools that a trained operator can use, for example, to manipulate the intensity scale to highlight bright or faint features, to evaluate the quality of the data as it is being obtained, or to check for saturation. For example, see Figure 5.

The RUCCD is a very flexible instrument, given eight filter choices, a wide range of possible CCD readout times, and the frame size and binning. MaxIm DL is a powerful data acquisition and analysis package that can fully harness these capabilities. However, this complexity could make it difficult to use the instrument in a time-pressure situation. We have therefore written a small number of simplified MaxIm DL scripts (currently 11) that focus on the most interesting scientific and calibration observations that might be made, but that retain some necessary operator control. For example, one script will cycle through the polarizers after the operator has initially optimized the exposure time.

The computer running the RUCCD in the control room does not have an internet connection to the outside world. The data is therefore transferred using an external hard drive to a second computer that has an edu connection for downloading by outside astronomers.

3.5 RUCCD Data Analysis and Calibration

The RUCCD data is analyzed using standard packages in IRAF.

A significant effort has gone into calibrating the RUCCD using standard stars, bright emission line sources (such as Campbell's hydrogen star and symbiotic stars), smooth ESO spectral standards, and polarized and unpolarized stars [41]. This activity is ongoing. Observations of the same star spaced a year apart show no change in the measured flux, demonstrating that the instrument is very robust.

We have also been improving the response to test and real ToO triggers. The goal is to get the AEOS telescope on to a burst location as soon as possible after the coordinates are issued. In addition to being critical for optimizing the scientific return of our experiment, this provides valuable rapid-response training for the telescope personnel, as needed for their other missions.

4. SAMPLE IMAGES

In Figures 6 - 9 we show some sample images from our calibration observations. They were all taken under mediocre seeing ($\sim 1.1''$), and before we had a full mount model to allow a proper tracking of our targets. However, the results are still quite impressive. These illustrate that our instrument is working as planned; in fact, it is better than expected in both optical and detector quality. To highlight the raw capabilities of the RUCCD, these images have had minimal data processing beyond the binning in the camera. Hot pixels and cosmic rays have not been removed. False-color intensity coding has been used.

Figure 6 shows a raw image of Saturn taken in the V-band. The rings of Saturn just fit into the full field of view of the RUCCD at the Coudé focus.

Figure 7 shows the Eskimo Nebula (NGC 2392) – a planetary nebula – taken in the R_c-band. The nebula has brighter irregular inner rings of emission and a fainter outer ring that is more circular but clumpy.

Figure 8 shows a portion of the globular cluster M79 (NGC 1904) taken in the I_c-band. The core of the cluster is towards the bottom right of the image. This image nicely illustrates the high quality and uniformity of the CCD, and that the focus is good across the whole field of view.

Figure 9 shows a full-field image of Campbell's hydrogen envelope star (BD +30 3639 or HD 184738), a compact ($7''$ across) planetary nebula taken using our grism. The object in the center of the image is the undispersed star and envelope (which appears as a ring). These are dispersed in the image both above and (faintly) below. The dispersed ring remains sharp because it is dominated by the line emission from hydrogen (Hα at 656.3 nm). The spectrum of the central star also has strong emission lines. For example, the bright knot at the bottom part of the dispersed ring is primarily due to an ionized carbon line from the central star (C III at 569.6 nm) which is overlapping with the Hα from the ring. The peak in the center of the dispersed ring is also primarily due to a carbon line from the central star (C II at 657.8 nm).

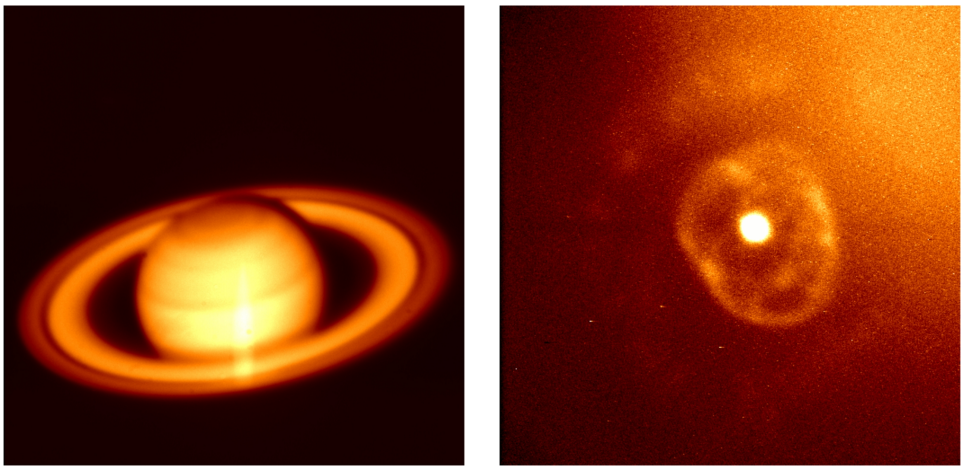

Figure 6: [Left] RUCCD V-band image of Saturn taken UT 2004-02-07:06:07:12. This is a raw image, with no data processing except for the 4×4 binning that was done in the camera, and the intensity color-coding. The exposure time was 70 milliseconds.

Figure 7: [Right] RUCCD R_c-band image of the Eskimo Nebula (NGC 2392) taken UT 2004-02-07:07:13:43. The image was binned 4×4 in the camera, and the dark current has been subtracted. The exposure time was 10 seconds.

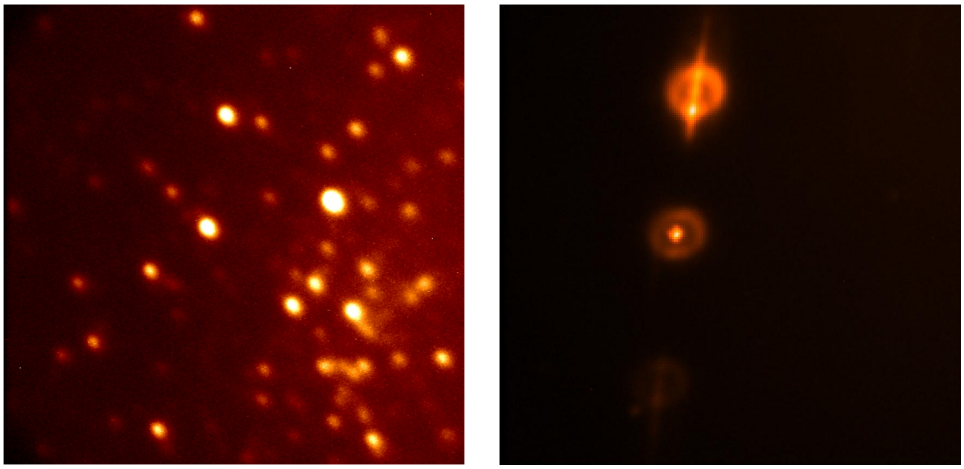

Figure 8: [Left] RUCCD I_c-band image of a portion of the globular cluster M79 taken UT 2004-02-07:08:07:43. The image was binned 4×4 in the camera, and the dark current has been subtracted. The exposure time was 10 seconds.

Figure 9: [Right] RUCCD grism image of Campbell's hydrogen envelope star (BD +30 3639 or HD 184738) taken UT 2004-05-10:14:33:42. The image was binned 10×10 in the camera, and the dark current has been subtracted. The exposure time was 2 seconds.

5. RUCCD GRB OBSERVATIONS

The RUCCD is fully operational, and has been certified to perform GRB Target of Opportunity observations with a high priority override. We expect to observe ~ 5 good bursts with the RUCCD per year, spending up to ~ 2 hours per burst. The primary goal of the project is to perform rapid observations that can be used to address the questions raised in §2.

The first burst that we called the AEOS telescope for rapid RUCCD observations was GRB 050416a. Un-

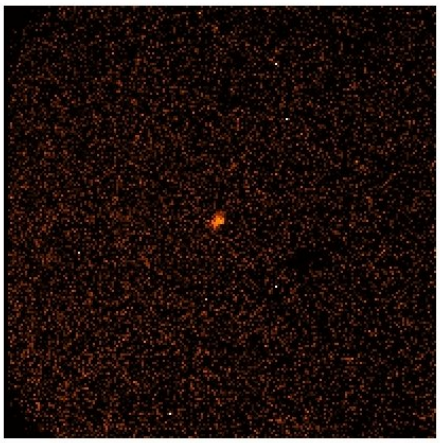

Figure 10: RUCCD I_c-band observation of the afterglow to GRB 051111 taken at 07:06:25 on 2005-11-11 (1.11 hours after the burst trigger). The flux of the afterglow at this time was $I_c = 16.9 \pm 0.2$.

fortunately, AEOS was down at that time. Telescope downtime and more often bad weather (e.g. GRBs 050607, 050712, 050713b, and 050820a) reduce the number of bursts that can be observed.

The first burst observed by the RUCCD was GRB 050906. This short burst did not have a convincing X-ray or optical counterpart. The ABC observed it, but did not detect a variable counterpart [42]. The RUCCD observed the galaxy IC 328 in the burst error box, but also did not see anything significant.

The first fading afterglow detected by the RUCCD was for GRB 051111, a long *Swift* burst [43] at a redshift of 1.55 [44]. Although immediate observations were requested, AEOS was performing a telescope software test that could not be interrupted. This meant that the first RUCCD observation did not take place until 32 minutes after the burst (the ABC was not available for this burst). However, the afterglow was still significantly detected, and was seen to fade over the next half hour. VRI photometry was taken, and a standard star was observed to check the flux calibration. Observations were stopped 1.1 hours after the burst due to concerns about the humidity (we were doing aperture observing throughout). At that time, the counterpart was at $V = 17.1 \pm 0.3$, $R_c = 17.5 \pm 0.2$, and $I_c = 16.9 \pm 0.2$. The corresponding I_c image is shown in Figure 10. Quick-look results for this burst were presented in a GCN Circular [45], and the full RUCCD results were added to the detailed ROTSE, *Swift*, and MDM observations [46].

6. SUMMARY

GRBs are the most energetic explosions in the Universe since the Big Bang. Significant progress has been made recently in understanding their nature. It appears that at least some of the bursts are related to energetic supernova explosions. However, there is much left to learn about these enigmatic objects. The RUCCD is fully functional in Coudé room 6 of the AEOS telescope. It will make good use of the unique capabilities of AEOS to perform a wide array of imaging, spectroscopic, and polarimetric studies of GRBs. It will be an important complement to *Swift* and the other ground and space-based observatories that are studying GRBs.

The versatile filter set and simple control system for the RUCCD makes it an instrument that the AEOS science community might find suited for their science related to other types of objects. The RUCCD is available to the Air Force and other visiting scientists for imagery, spectroscopy, and/or polarimetry observations with the AEOS telescope. A user manual has been written that explains the set-up, take-down, and operation procedures. Training can be provided to anyone who wants to use it, and we welcome discussions regarding its expanded use.

7. ACKNOWLEDGEMENTS

The smooth installation and operation of the RUCCD has been made possible through the extensive efforts and cooperation of the staff at the telescope, and we would like to thank everyone who has spent time helping us. Particular thanks for their help with our project go to John Africano, Spence Ah You, Paul Bellaire, Peter Figgis, John Flam, Tom Goggia, Nancy Ichikawa, Paul Kervin, Kevin Moore, Thomas Nakagawa, Karl Rehder, Lewis Roberts, David Talent, and Darius Vunck.

The US Air Force provides the telescope time, on-site support and 80% of the research funds for this AFOSR and NSF jointly sponsored research under grant number NSF AST-0123487.

8. REFERENCES

[1] Fishman, G. J., & Meegan, C. A. 1995, ARA&A, 33, 415.
[2] Van Paradijs, J., Kouveliotou, C., & Wijers, R. A. M. J. 2000, ARA&A, 38, 379.
[3] Mészáros, P. 2002, ARA&A, 40, 137.
[4] Klebesadel, R. W., Strong, I. B., & Olson, R. A. 1973, ApJ, 182, L85.
[5] Gehrels, N., et al. 2004, ApJ, 611, 1005.
[6] http://gcn.gsfc.nasa.gov/gcn/gcn_main.html
[7] Kouveliotou, C., et al., 1993, ApJ, 413, L101.
[8] Burrows, D. N., et al. 2005, Science, 309, 1833.
[9] Van Paradijs, J., et al. 1997, Nature, 386, 686.
[10] Kawai, N., et al. 2006, Nature, 440, 184.
[11] Frail, D. A., et al. 2001, ApJ, 562, L55.
[12] http://swift.gsfc.nasa.gov/
[13] Matheson, T., et al. 2003, ApJ, 599, 394.
[14] Kosugi, G., et al. 2004, PASJ, 56, 61.
[15] Panaitescu, A., et al. 2001, ApJ, 561, L171.
[16] Palmer, D. M., et al., 2005, Nature, 434, 1107.
[17] Lazzati, D., et al. 2005, MNRAS, 362, L8.
[18] http://space.mit.edu/HETE/
[19] Akerlof, C., et al. 1999, Nature, 398, 400.
[20] Vestrand, W. T., et al. 2005, Nature, 435, 178.
[21] Boër, M., et al. 2006, ApJ, 638, L71.
[22] Liang, E. P., Crider, A., Böttcher, M., & Smith, I. A. 1999, ApJ, 519, L21.
[23] Coburn, W., & Boggs, S. E. 2003, Nature, 423, 415.
[24] Rutledge, R. E., & Fox, D. B. 2004, MNRAS, 350, 1288.
[25] Covino, S., et al. 1999, A&A, 348, L1.
[26] Wijers, R. A. M. J., et al. 1999, ApJ, 523, L33.
[27] Rol, E., et al. 2000, ApJ, 544, 707.
[28] Greiner, J., et al. 2003, Nature, 426, 157.
[29] Heise, J., et al. 2001, in Gamma-Ray Bursts in the Afterglow Era, Springer, 16.
[30] Lamb, D. Q., Donaghy, T. Q., & Graziani, C. 2005, ApJ, 620, 355.
[31] Bishop, J., et al., 1999, AMOS Technical Conference, 8.
[32] Akerlof, C., et al. 2006, these proceedings.
[33] http://www.hardin-optical.com/
[34] http://www.atmel.com/
[35] http://www.ccd.com/
[36] http://www.dfmengineering.com/
[37] http://www.optecinc.com/astronomy/products/filters.html
[38] http://www.edmundoptics.com/
[39] http://www.spectra-physics.com/
[40] http://www.cyanogen.com/
[41] Silverman, J. 2005, Rice University Senior Thesis.
[42] Swan, H. F., & Smith, I. 2005, GCN #3936.
[43] Sakamoto, T., et al. 2005, GCN #4248.
[44] Hill, G., et al. 2005, GCN #4255.
[45] Smith, I. A., & Swan, H. F. 2005, GCN #4267.
[46] Yost, S. A., et al. 2006, ApJ, submitted.